Editorial Manager(tm) for Bulletin of Earthquake Engineering
Manuscript Draft

Manuscript Number: BEEE508R1

Title: Extensive characterization of Italian accelerometric stations from HVSR ambient vibration measurements

Article Type: SI: Italian strong motion database ITACA

Keywords: HVSR; ambient vibration measurements; strong motion database

Corresponding Author: Rodolfo Puglia

Corresponding Author's Institution: Istituto Nazionale di Geofisica e Vulcanologia

First Author: Rodolfo Puglia

Order of Authors: Rodolfo Puglia;Dario Albarello;Antonella Gorini;Lucia Luzi;Sandro Marcucci;Francesca Pacor

Abstract: This paper describes the analyses of the single-station ambient vibration measurements performed on the Italian accelerometric network to detect site resonance phenomena potentially affecting earthquake recordings. The use of low cost, high quality microtremor measurement can be helpful to discriminate among soil classes, since several classification schemes based on resonance frequencies were proposed in the last decades. Operatively, in the framework of the Italian Strong Motion Database project (DPC-INGV 2007-2009 S4; http://esse4.mi.ingv.it), soil resonance frequencies have been evaluated from more than 200 ambient vibration measurements in correspondence of accelerometric stations included in ITACA (http://itaca.mi.ingv.it/ItacaNet/). The noise recordings have been analyzed using the same numerical protocol in order to standardize the results. Particular attention has been paid to evaluate the quality of measurements and to develop an on-purpose mathematical tool to automatically estimate the peaks in the horizontal-to-vertical spectral ratio (HVSR) curve. The reliability of the resonance frequencies from HVSR has been tested by comparing estimates provided by independent methods (modeling or earthquake recordings). The test confirmed the reliability of the microtremor HVSR for assessing the resonance frequencies of the examined sites.

Response to Reviewers: Responses to reviewers are in attachment

BULLETIN OF EARTHQUAKE ENGINEERING

Title: **Extensive characterization of Italian accelerometric stations from HVSR ambient vibration measurements**

Submitted: January, 2011

Authors: R. Puglia* (1), D. Albarello (2), A. Gorini (3), L. Luzi (1), S. Marcucci (3), F. Pacor (1)

(1) Istituto Nazionale di Geofisica e Vulcanologia, Milano, Italy
(2) Dept. of Earth Sciences, University of Siena, Siena, Italy
(3) Dipartimento della Protezione Civile Nazionale, Roma, Italy

* corresponding author details:
Dr. Rodolfo Puglia
Istituto Nazionale di Geofisica e Vulcanologia
Sezione di Milano-Pavia
via Bassini 15
20133 Milano, Italy
ph.: (+39) 02 23699259
fax: (+39) 02 23699267
email: rodolfo.puglia@mi.ingv.it

Extensive characterization of Italian accelerometric stations from HVSR ambient vibration measurements

R. Puglia[(1)], D. Albarello[(2)], A. Gorini[(3)], L. Luzi[(1)], S. Marcucci[(3)], F. Pacor[(1)]

(1) Istituto Nazionale di Geofisica e Vulcanologia, Milano, Italy

(2) Dept. of Earth Sciences, University of Siena, Siena, Italy

(3) Dipartimento della Protezione Civile Nazionale, Roma, Italy

Abstract

This paper describes the analyses of the single-station ambient vibration measurements performed on the Italian accelerometric network to detect site resonance phenomena potentially affecting earthquake recordings. The use of low cost, high quality microtremor measurement can be helpful to discriminate among soil classes, since several classification schemes based on resonance frequencies were proposed in the last decades. Operatively, in the framework of the Italian Strong Motion Database project (DPC-INGV 2007-2009 S4; http://esse4.mi.ingv.it), soil resonance frequencies have been evaluated from more than 200 ambient vibration measurements in correspondence of accelerometric stations included in ITACA (http://itaca.mi.ingv.it/ItacaNet/). The noise recordings have been analyzed using the same numerical protocol in order to standardize the results. Particular attention has been paid to evaluate the quality of measurements and to develop an on-purpose mathematical tool to automatically estimate the peaks in the horizontal-to-vertical spectral ratio (HVSR) curve. The reliability of the resonance frequencies from HVSR has been tested by comparing estimates provided by independent methods (modeling or earthquake recordings). The test confirmed the reliability of the microtremor HVSR for assessing the resonance frequencies of the examined sites.

1. Introduction

Analysis of ambient vibration (microtremor) measurements provides useful indications about seismic response of the subsoil. In particular, some authors (Nogoshi & Igarashi, 1971; Nakamura, 1989; Bard, 1999) assessed that the presence of a sharp peak in the curve representing the average ratios of Horizontal to Vertical spectral components of ambient vibrations as a function of frequency (hereafter HVSR from "Horizontal to Vertical Spectral Ratios") is indicative of a significant shear wave impedance contrast in the subsoil. Furthermore, empirical evidence (SESAME, 2005; Haghshenas *et al.*, 2008) and theoretical modelling (e.g., Lunedei and Albarello, 2010) suggest that, in the presence of a layered flat subsoil, HVSR peaks show a good correspondence with SH fundamental resonance frequencies of the subsoil. This frequency roughly corresponds to the ratio $V_S/4H$, where V_S is the average shear waves velocity of the shallow soft layer overlying a more rigid formation at a depth H. The amplitude of the peak is also indicative (just in relative and merely qualitative terms) of the strength of the

seismic impedance contrast responsible for the resonance effects (e.g., Albarello and Lunedei, 2011).

Despite of the fact that a general agreement exists about the above major features, an univocal physical interpretation of microtremor HVSR is still lacking and, for this reason, physical interpretation of the HVSR curve is a controversial point. A basic aspect that needs to be clarified is the relative amount of body and surface waves components in the ambient vibration wavefield. Bonnefoy-Claudet *et al.* (2008) have demonstrated, for the 1D horizontally layered sites analyzed in their study, that, around an HVSR peak, the horizontal polarization of the Rayleigh waves is fulfilled in the case of high impedance contrast ($Z_C > 4$), but is not always satisfied if low or moderate contrasts are present. In these latter cases, the authors have found that, depending on the investigated site, alternatively higher Rayleigh-wave modes or S-wave or Love waves could be dominant. Recently, Albarello and Lunedei (2010) have observed, for the subsoil structures tested in their study, characterized by a single sharp impedance contrast, that vibrations at frequencies above an HVSR peak are dominated by surface waves, while body waves are predominant around and below the fundamental frequency. These considerations imply that around a fundamental frequency, a mixture of seismic phases exists whose relative contributions mainly depend on the subsoil structure. Despite of this, however, both empirical evidence and theoretical considerations show that the distribution of noise sources and their intensity only weakly affects the position of the HVSR peak and its correspondence with the S-waves resonance frequency. On the contrary, the noise sources distribution may significantly influence the amplitude of the HVSR curve (SESAME 2005; Lunedei and Albarello, 2010). This could explain the lack of a strict relationship between the HVSR curve and the amplification function around a fundamental frequency of the site.

The fact that ambient vibrations can provide cheap and effective information about basic seismic properties of a site (presence of resonance phenomena and frequencies characterizing such resonance) attracted a considerable interest of the scientific community in the HVSR technique, especially for extensive applications such as seismic microzonation (among others, Lermo and Chávez-García, 1993; Lachet *et al.*, 1996; Bonilla *et al.*, 1997; Parolai *et al.*, 2001; D'Amico *et al.*, 2008; Manakoua *et al.*, 2010). Another important field of potential application of HVSR measurements is the extended characterization of accelerometric networks. It is well known that, being qualitative in nature, geologic surveys alone do not allow a correct seismic characterization of a site. On the other hand, when the number of accelerometric sites is of the order of hundreds, the application of intensive seismic surveys (e.g., cross-hole or down-hole) requires funds well beyond those commonly allocated on purpose. Thus, for seismic networks characterization, cheap extensive surveys carried on by using single station ambient vibration measurements could provide a clue for site effects estimation, at least to identify sites where seismic resonance phenomena could occur in the frequency range of potential engineering interest (cf. Bonilla *et al.*, 1997). Such surveys, however, being devoted to the characterization of a sparse network, requires application of a number of independent crews operating in quite different situations. In collecting data provided in this way, it become mandatory developing standardized post processing and validation procedures making all the data comparable. Of great importance it is also the identification of experimental parameters useful for a correct (whether rough) seismic characterization of sites. In this regard, microtremor measurements providing direct information on the

resonance soil frequencies could allow the application of classification schemes alternative to those based on the single $V_{S,30}$ (average shear wave velocity of the upper 30m). Actually, several alternative classification schemes have been proposed (e.g., JRA, 1980; Zhao *et al.*, 2006; Fukushima *et al.*, 2007; Cadet *et al.*, 2008; Luzi *et al.*, this issue) that are based on the use of fundamental/predominant resonance frequency (f_0) by alone or in parallel to the $V_{S,30}$. The use of both f_0 and $V_{S,30}$ allows to take in account, although in an indirect way, for the soil thickness, the parameter invoked by many authors as the principal deficiency imputable to classifications based on the single $V_{S,30}$. Furthermore, the identification of actual reference sites (i.e., sites where no amplification of local ground motion is expected as effect of local stratigraphic and morphologic configuration) is of paramount importance in seismic networks characterization and, also in this case, HVRS analyses could be of great help (among others, Steidl *et al.* 1996; Chávez-García *et al.*, 2002; Cadet *et al.*, 2010).
Standardized post-processing/validation protocols particularly devoted to the identification of site resonance frequencies are described that were developed at the sites of the Italian Accelerometric Network (RAN) managed by the National Agency of Civil Protection (hereafter DPC - *Dipartimento della Protezione Civile*). In particular, in the framework of the Italian Strong Motion Database project (DPC-INGV S4 2007-2009; http://esse4.mi.ingv.it), more than 500 stations were documented by new detailed monographic reports published in the ITalian ACcelerometric Archive (ITACA, http://itaca.mi.ingv.it/ItacaNet/). These monographs were designed to help the user in getting the available information about the morphologic, geologic, seismic and geotechnical characteristics of the site where the instrument was installed. In particular, the monograph includes the section "Microtremor H/V spectral ratio", which focuses on the analysis of the ambient vibration measurements. In the following sections, details concerning the experimental measurements are described together with the numerical protocol adopted to processing and validating measurements provided by the extensive HVSR survey provided by public and private companies on behalf of DPC . Then, particular attention is paid to the evaluation of the quality of the measurement and to develop specific algorithms aimed to identify the HVSR curve peaks and their band-width. Finally, fundamental resonance frequencies estimated from ambient vibration measurements are compared at about 20 sites with independent estimates in order to evaluate the reliability of the procedure.

2. Dataset description and processing procedure

On behalf of the Italian Agency of the Civil Protection (DPC), 156 microtremor measurements were executed at RAN stations (displayed as squares in Fig. 1) using LE-3D/5s sensors. This sensor is theoretically capable to record oscillations in the 0.2-40Hz frequency range. Furthermore, additional 67 microtremor measurements were collected from different research institutions (displayed as triangles in Fig. 1), recorded using LE-3D/5s (50 sites) and Mark L4C-3D (8 sites) sensors, and Tromino (9 sites) instruments. The duration of DPC measurements is, on average, about 3 hours – only in one case is lower than 60 minutes (50 minutes at the station PTZ) – and the sampling is fixed at 125 Hz. The measurements collected from other institutions are shorter: on average 60 minutes – only in two cases the length is less than 20 minutes (16 at MTC and 18 at CLC) – while the sampling spans between 100 and 200 Hz.

Since most of these measurements were carried on before the project by independent subjects, the experimental protocol was not fixed and standardized in advance. Thus, in the following, single field protocols will not described in details.

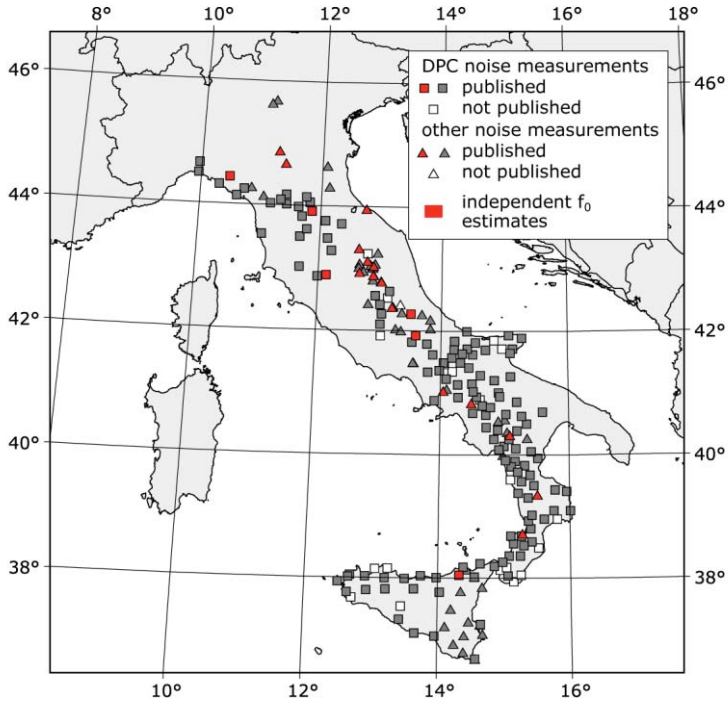

Fig. 1 - Map of the RAN stations analyzed in terms of microtremor measurements. Those provided by the National Agency of Civil Protection (DPC) are displayed as squares. The red color evidences the sites were independent estimates of f_0 are available (such as: from 1D simulations and/or horizontal-to-vertical spectral ratio of earthquakes).

In order to make these measurements comparable, all the records were processed through the same numerical approach. Preliminarily, a 1st order baseline correction and a 4th order acausal Butterworth band-pass filtering were applied to each time series. Each record was then subdivided in windows and the relevant minimum expected f_0 was defined following the criteria recommended in the project SESAME (2005). For instance, the window length was fixed to 20 seconds when the recording duration is lower than 30 minutes, and to 50 seconds in the other cases. Consequently, the minimum expected f_0 assumes the values of 0.5 and 0.2 Hz respectively. When the recording durations were longer than 100 minutes, the window was often extended to 100s. However, the minimum expected f_0 was always set to a value equal to or higher than the lower frequency recordable by the instrument. Therefore for longer recording durations made with LE-3D/5s sensors, it was also set to 0.2 Hz. The corners of the above-mentioned band-pass filter were fixed to half of the minimum expected f_0 and to 20 Hz. A 1st order baseline correction and a 5% cosine taper was applied to each window and the Fourier spectra were calculated and smoothed through the Konno and Ohmachi (1998) algorithm, fixing the relevant parameter b to 40. The HVSR values for each window were calculated as the ratio between the vector summation of the Fourier spectra of horizontal components and the spectrum of the vertical component. Lastly, obtained HVSR curves were averaged out considering a log-normal distribution of amplitudes to obtain the mean HVSR curve along with the relevant 68% confidence interval. Windows exhibiting large

transients were generally excluded from the analysis; these windows were visually identified from the velocity time series and from the single window Fourier spectra and spectral ratio.

For each microtremor measurement, a report was generated and published in ITACA on the station monograph under the section "Microtremor H/V spectral ratio" (Fig. 2). In this report, details about the measurement and the parameters adopted for the analysis are reported (Fig. 2a), such as the duration of the recording, the sensor model, the minimum expected f_0, the band pass corners, etc... In order to make the user aware of the basic features of the ambient vibration measurement available at the site, results are displayed in terms of: i) unfiltered smoothed Fourier spectra for each component (Fig. 2b), ii) HVSR time histories relevant to each component (Fig. 2c), iii) rotated HVSRs, calculated on the azimuthally projected horizontal components (Fig. 2d), iv) mean HVSR (Fig. 2e) and v) SESAME criteria indicating the degree of reliability of the HVSR peaks (Fig. 2f).

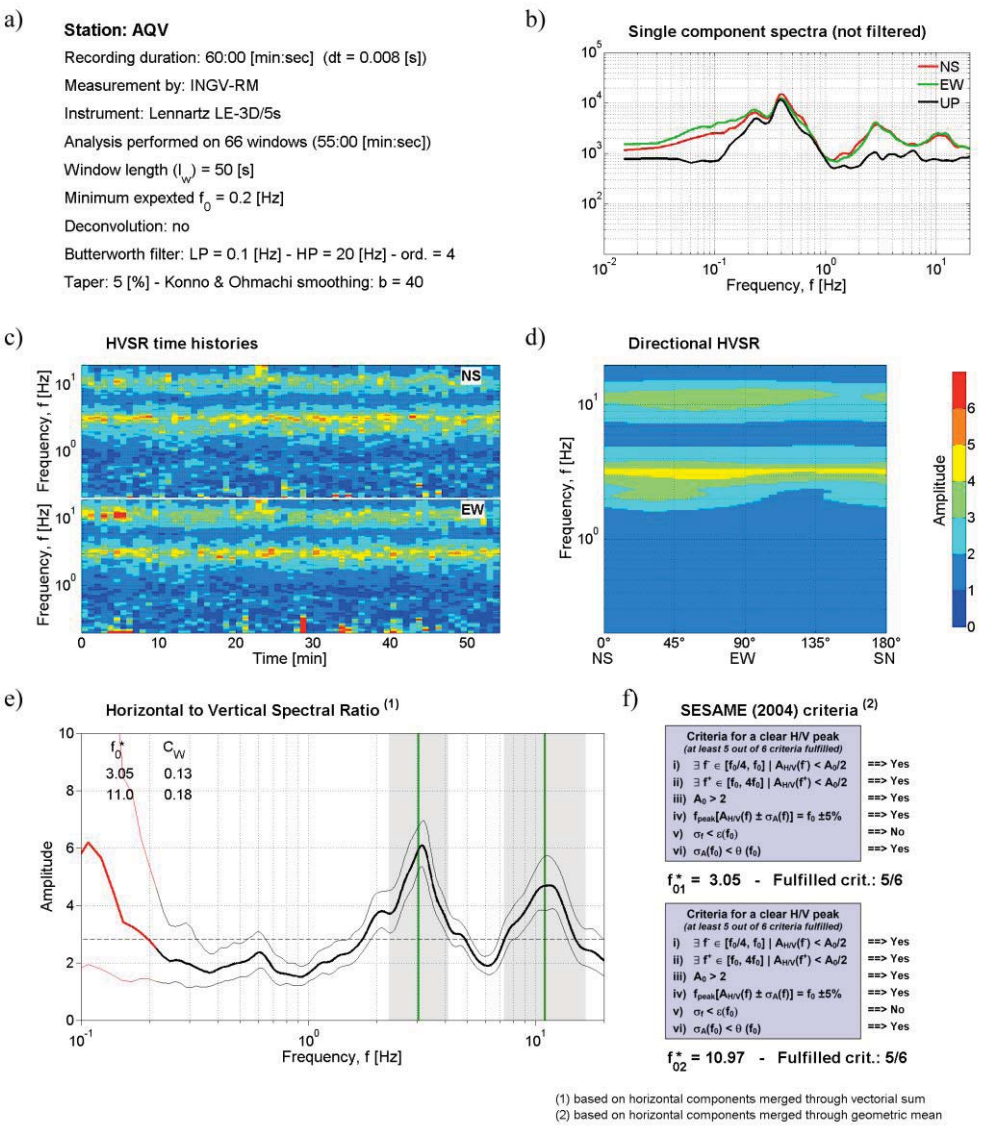

Fig. 2 - Example of a microtremor measurement report published on station monographs of ITACA: a) information about the measurement and processing parameters; b) smoothed-not filtered Fourier spectra (in this case, they are expressed in counts); c) HVSR time histories; d) HVSR azimuthal variations; e) mean HVSR (red lines evidence the portion of the ratios lower than the minimum expected f_0); f) SESAME European project (2005) reliability criteria for the peaks identified in the HVSR.

3. Criteria for the identification of reliable HVSR curves

The main goal of the technical reports published on ITACA is to provide the end-user with the information about the quality of the microtremor measurement and the reliability of the HVSR peak, if any. In order to provide an immediate indication about the quality of the single measurement and preventing misinterpretation of low-quality measurements, a reliability classification scheme was developed in the frame of the seismic microzoning activities following the 2009 L'Aquila earthquake by Albarello *et al*. (2011). This classification, is more conservative than the one proposed by the SESAME group (SESAME, 2005), since it includes more criteria. Albarello *et al*., 2011 defines three classes:

- class A: trustworthy and interpretable HVSR curve, it represents a reference measurement that can be considered by itself for the site of concern;
- class B: ambiguous HVSR curve, should be used with caution and in case of coherency with other measurements performed nearby;
- class C: poor quality HVSR curve (hardly interpretable), to be discarded.

Criteria used to classify measurements of class A are (Albarello *et al*., 2011):

1. effective duration of the analyzed record (cf. Fig. 2a): it should include at least, 15 minutes of useful registration;
2. physical plausibility of the Fourier spectra (cf. Fig. 2b): in particular, a HVSR peak should be marked by a significant lowering of the vertical spectral component amplitudes;
3. absence of artefacts (cf. Fig. 2b): man made disturbances (e.g. electromagnetic noise or peaks of industrial origin) could be often recognized in the Fourier spectra as monochromatic disturbances;
4. stationary of HVSRs with time (cf. Fig. 2c): the curves show a persistent shape for at least the 30% of the duration of the record;
5. isotropy of HVRSs (cf. Fig. 2d): the azimuthal amplitude variations do not exceed the 30% of the peak; larger variations could indicate an interaction with a nearby structure or complex site effects;
6. statistical robustness: SESAME (2005) criteria "for a reliable H/V curve" are fulfilled.

A measurement belongs to class B if one or more of the previous conditions are not fulfilled. Class B measurements degrade to class C if:

- a rising drift exists from low to high frequencies (cf. Fig. 2b), that indicates a tilting of the instrument (Forbriger, 2006);
- man-made mono-harmonic disturbances affect several frequencies in the frequency range of interest.

In particular, in ITACA, 193 HVSR measurements were published out of a total of 223 available: 73 of them were classified as A, 99 as B and 21 as C. Please notice that some Type C. measurements were anyway included by considering them at least weakly informative.

Figure 2 is the report relevant to a class B measurement where, in correspondence of the two peaks at 3 and 11 Hz, the significant lowering of the vertical Fourier spectra is absent. It should be noticed, that around 0.1 Hz another peak is present in the HVSR (cf. Fig 2e). It is represented in red, because it falls beyond than the minimum expected f_0 (cf. Fig 2a), but, around this peak, although the records were acquired with an LE-3D/5s sensor, Fourier spectra do not present any drift

and the energy content of the acquired signals seems adequate (cf. Fig 2b). Therefore, observation of the microtremor measurement report of Figure 2 suggests that this low frequency peak can hardly be considered and artifact. Figure 3 and 4 show class B measurements for which HVRS temporal non-stationarity and non-isotropy were observed, respectively. In Figure 5 a class C measurement is shown, where the record is clearly contaminated by anthropic noise, which causes a spurious peak in the HVSR at 4.6Hz. However, in this case, the presumably man-made peak at 4.6Hz does not affect the peak at 2Hz, which could be therefore considered reliable. In the ITACA database this report and the relevant f_0 value (2.2Hz) are published with the warning of class C measurement. About 30 measurements were not published because of instrument malfunctioning, evidenced by instrumental noise present in the Fourier spectra, or because of the presence of strong anthropic monochromatic disturbances in the records, just in correspondence of the fundamental frequency.

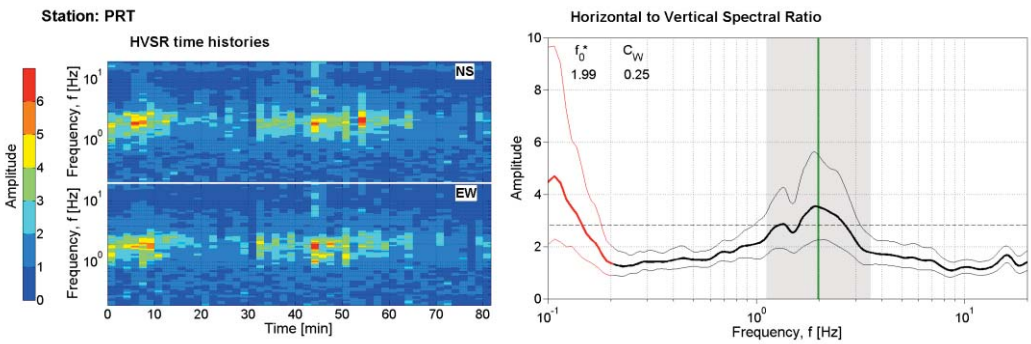

Fig. 3 - Class ‘B’ HVSR affected by temporal non-stationarity.

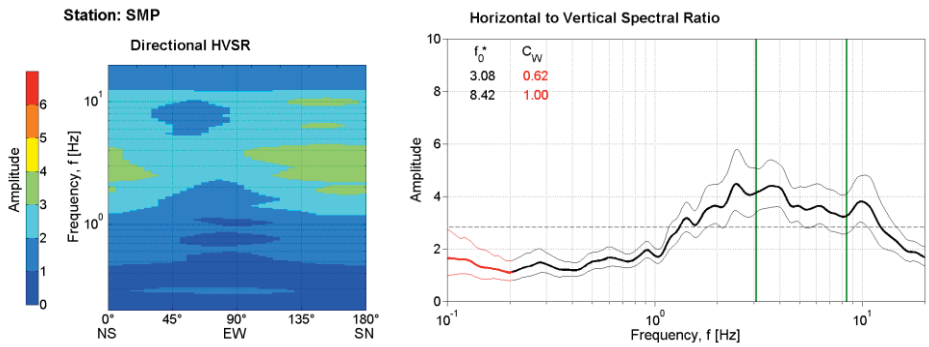

Fig. 4 - Class ‘B’ non-isotropic HVSR.

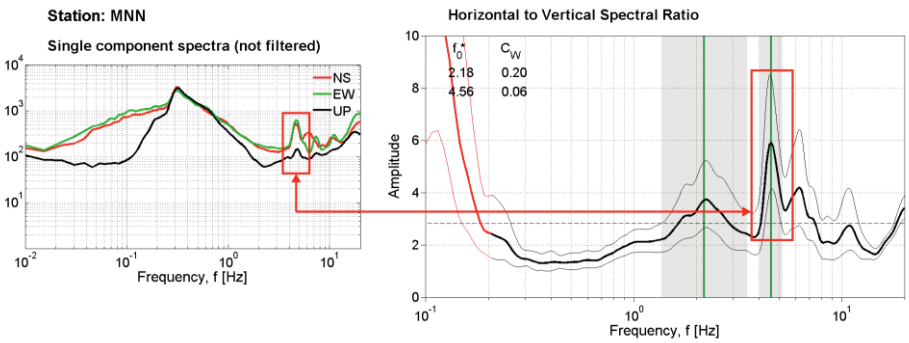

Fig. 5 - Class ‘C’ HVSR affected by anthropic mono-harmonic disturbances (Fourier spectra are expressed in counts).

4. Estimate of the site resonance frequencies

The criteria described in the previous paragraph are used to assess the reliability of the HVSR curve. In order to physically interpret the curve in terms of "absence/presence" of resonance phenomena, two situations should be distinguished:

- type 1 (possible resonance): the HVSR curve presents at least one clear peak in the frequency range where the measurement could be considered reliable;
- type 2: the HVSR curve does not present any clear peak in the frequency range where the measurement could be considered reliable.

In order to provide such distinction, an automatic procedure was implemented to identify the peaks in the microtremor HVSR curve and to evaluate their reliability in terms of the SESAME (2005) criteria "for a clear H/V peak". It is worth noting that the automatic detection of the maxima of an empirical curve is not an easy task, due to a number of possible local irregularity of the curve. Thus, an on-purpose numerical procedure was developed that warrants the "robustness" against a possible "fake" identification. The output of this procedure is represented by one or more frequencies at which a peak occurs in the HVSR curve: these are respectively termed f_0^*, if only one peak is detected, otherwise f_{01}^*, f_{02}^*, etc., from the lowest to the largest frequency (cf. Fig. 2e-f).

Whenever an f_0^* is detected, its reliability is tested by the application of the SESAME criteria, shown in the station monograph (cf. Fig. 2f). Following the criteria explained in the previous section, if the HVSR curve is judged trustworthy in the neighborhood of the fundamental frequency, f_0^*, (type 1), its value is published on the ITACA database as f_0. A value of zero assigned to an f_0 means that the relevant HVSR curve is reliable but flat in the considered range of frequencies (type 2). Currently, in ITACA, more than 140 stations are associated to one f_0 value, and about 70 of them provide a flat HVSR curve. In particular, 73 out of these 140 measurements belong to class A, 65 to class B and 5 to class C. In case of more than one reliable f_0^*, it was decided to provide the end-user a single value of f_0 corresponding to the HVSR peak closer to the range of frequencies from 1 to 5Hz, typical of ordinary buildings in civil engineering design.

4.1 Peaks detection

The peak detection procedure needs, as input, the curve $A(f)$, i.e. the HVSR curve defined between f_{MIN} and f_{MAX}, where f_{MIN} is the minimum value of interest for f_0 (or the lowest frequency attainable with the relevant experimental tool) and f_{MAX} is 20Hz (i.e. a value considered to bound resonance phenomena of possible engineering interest). A set of parameters is also introduced to drive the selection of maxima *N*, *L*, *a*, *M*, *p*, A' and *R* (Table 1), whose meaning will be explained in the following. With the exception of A', which depends on the method used to merge horizontal components, the other parameters were assigned after applying a trial and error approach. Statistical tests were performed in order to assign to the

parameters listed in Table 1 the most suitable value, which led to the safe selection of acceptable peaks.

The peak detection procedure could be summarized through the following steps:

1. re-sampling of $A(f)$ in N points ($\bar{f}_i$) equally-spaced in a logarithmic scale, to obtain $A(\bar{f})$; this step is necessary since HVSR curves were provided with different sampling in the frequency domain;
2. selection of M frequencies $\bar{f}_{i_m}$, with $1 < m < M$, being each *m-th* selected frequency a starting point of an iterative process which leads to the identification of a local maximum of the HVSR curve; in the analysis described below, the M starting frequencies were equally-spaced in a logarithmic scale in the range [f_{MIN} , f_{MAX}].

This identification is provided through the evaluation of the centres of mass of the $A(\bar{f})$ function in specified intervals.

In particular, each starting frequency $\bar{f}_{i_m}$, where $1 < i_m < N$, is associated to the interval [$\bar{f}_{i_m-\Delta}$; $\bar{f}_{i_m+\Delta}$]. The parameter Δ, which is used to define the above-mentioned interval, generally assumes the value of $L/2$, except when is close to the $A(\bar{f})$ limits f_{MIN} or f_{MAX}. In this latter case, if $\bar{f}_{i_m-\Delta} < f_{MIN}$ or $\bar{f}_{i_m+\Delta} > f_{MAX}$, the parameter Δ is reduced (to $i_m - 1$ or $N - i_m$, respectively).

Table 1 - Coefficients adopted for the estimation of the HVSR curve local maxima and their relevant C_W.

N	400
L	60
a	10
M	8
p	1.3
A’	$2 \cdot \sqrt{2}$
R	0.8

The frequency corresponding to a local maximum of the function $A(\bar{f})$ is estimated through an iterative process using the equation:

$$f_Y = \sum_{j=i_m-\Delta}^{i_m+\Delta} A^a(\bar{f}_j) \cdot \bar{f}_j \Bigg/ \sum_{j=i_m-\Delta}^{i_m+\Delta} A^a(\bar{f}_j) \qquad \text{(Eq. 1)}$$

where a is an exponent to be applied to the $A(\bar{f})$ curve. This exponent aims at providing a larger weight to the largest HVSR values as the most probable candidate to be a maximum. The frequency f_Y corresponds to the center mass of the set of the $A^a(\bar{f})$ values within the interval [$\bar{f}_{i_m-\Delta}$; $\bar{f}_{i_m+\Delta}$]. f_Y is then associated to the closest frequency used to resample the HVSR and its index assumes values belonging to the interval [1; N]. This index is hereinafter termed *center of mass index*, k_m, relative to the *m-th* starting frequency. While the center of mass index is different from the starting frequency index (i_m), i_m has to be upgraded with the current value of the center of mass index and another iteration has to be carried out adopting new interval limits for the summations in Equation 1. As previously stated, when $\bar{f}_{i_m-\Delta} < f_{MIN}$ or $\bar{f}_{i_m+\Delta} > f_{MAX}$, the parameter Δ is

reduced. The frequency $\bar{f}_{k_m}$ at which the iteration stops, represents a local maximum of A($\bar{f}$) and is identified as f_0^*.

The process is repeated for the *M* starting frequencies $\bar{f}_{i_m}$. In this way, each frequency tends to a local maximum (Fig. 6). At the end of the processes, the local maximum f_0^* will be discarded when: a) it falls outside the interval [$p \cdot f_{MIN}$; f_{MAX}/p], where p (> 1) is *a-priori* selected to avoid the closeness of f_0^* to the curve limits, f_{MIN} and f_{MAX}; b) the amplitude of HVSR at f_0^* is smaller than an amplitude threshold A'.

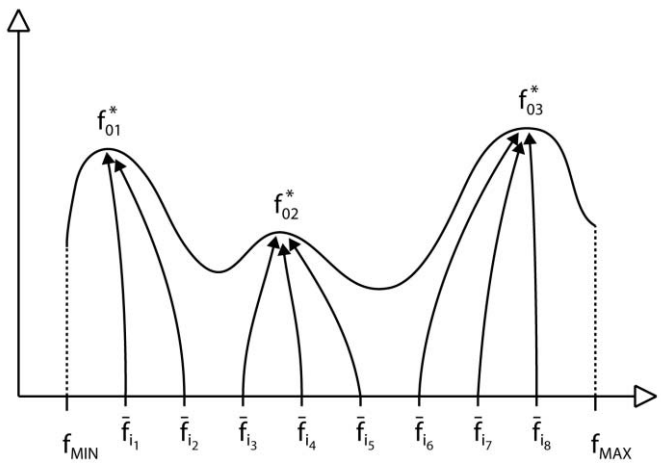

Fig. 6 - Iterative processes of migration of $\bar{f}_{i_m}$ to a local maximum. The figure is drawn considering *m*=8.

4.2 Band-widths estimation

A curve A($\bar{f}$) could be characterized by one peak f_0^* or more. In this last case f_{01}^* will indicate the peak at the lowest frequency above f_{MIN} and f_{02}^*, f_{03}^*,… will, indicate maxima at higher frequencies. To evaluate sharpness of the HVSR curve nearby each of these values, a quality parameter C_W is introduced. For each f_0^* the C_W is calculated which estimates the band-width associated to the corresponding peak. The parameter C_W, is evaluated through an iterative process. At the base of this process there is the function A($\bar{f}$) defined in the range of frequencies [$\bar{f}_{q-\Delta_1}$;$\bar{f}_{q+\Delta_2}$], where q is the index corresponding to f_0^* and $\Delta_1 = \Delta_2 = [1, 2, \ldots]$ increase at each iteration. For each iteration, two areas are calculated: a) the area R_C of the rectangle circumscribed to the function A($\bar{f}$) and b) the area R_L, i.e. the integral of the same function, as in Figure 7. When an extreme of the interval [$\bar{f}_{q-\Delta_1}$;$\bar{f}_{q+\Delta_2}$] coincides with f_{MIN} or f_{MAX}, the band will be expanded only in the other direction. The process will interrupt when R_C/R_L reaches the fixed value *R* or when the integration interval is equal to [f_{MIN}; f_{MAX}]. The identified interval [$\bar{f}_1$; $\bar{f}_2$], corresponding to the process interruption, is used to define C_W as:

$$C_W = \frac{\log\left(\bar{f}_2/\bar{f}_1\right)}{\log\left(f_{MAX}/f_{MIN}\right)} \qquad \text{(Eq. 2)}$$

which could thus assume values in the interval]0; 1]. The smaller the C_W, the sharper will be the peak. Smaller C_W values will indicate sharp well defined peaks. When a f_0^* is identified, the corresponding C_W is provided on the station monograph (cf. Fig. 2e).

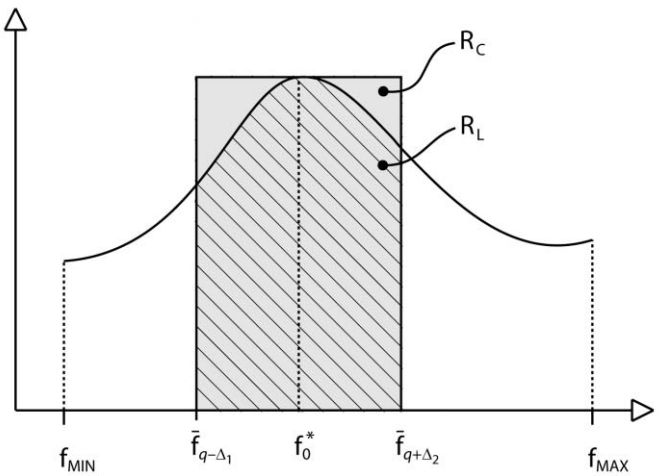

Fig. 7 - Approach used to estimate the band-width associated to the peak at f_0^*.

4.3 Examples

In Figure 8 and Table 2 examples of peak detection and C_W evaluation are shown at several RAN stations. In Table 2, for each f_0^* detected for the HVSR curves of Figure 8, the following parameters are reported: i) the band-width limits $\bar{f}_1$ and $\bar{f}_2$; ii) $C_W/A\left(f_0^*\right)$, where $A\left(f_0^*\right)$ represent the amplitude of the average HVSR at f_0^*; iii) *S*, i.e. the number of fulfilled SESAME criteria "for a clear H/V peak" (SESAME, 2005). The HVSR curve relative to the station ACR has lower values than the threshold A' (evidenced by the dashed line) therefore no peaks are detected (cf. Fig. 8). The HVSR curve relative to the station ALD is characterized by a f_0^* associated to a band-width, C_W, larger than 0.6 (cf. Tab. 2) and, thus, its limits are not reported in Figure 8. In the case of station ANT a clearer peak is observed around 2Hz, associated to a small $C_W/A\left(f_0^*\right)$ of 0.08. In general, a threshold value of 0.10 could be considered acceptable to discriminate sharp peaks. The HVSR of station AQV is characterized by two resonance frequencies. The first peak occurs at about 3Hz and the second at 11Hz. In this case the lowest frequency value f_0^* is published in ITACA as fundamental resonance frequency. However, the second peak, probably connected to a shallow impedance contrast, seems also reliable (cf. Figure 2). The information provided in the report allows the end-user to have additional elements to judge both the quality of the measurement and the reliability of the peaks.

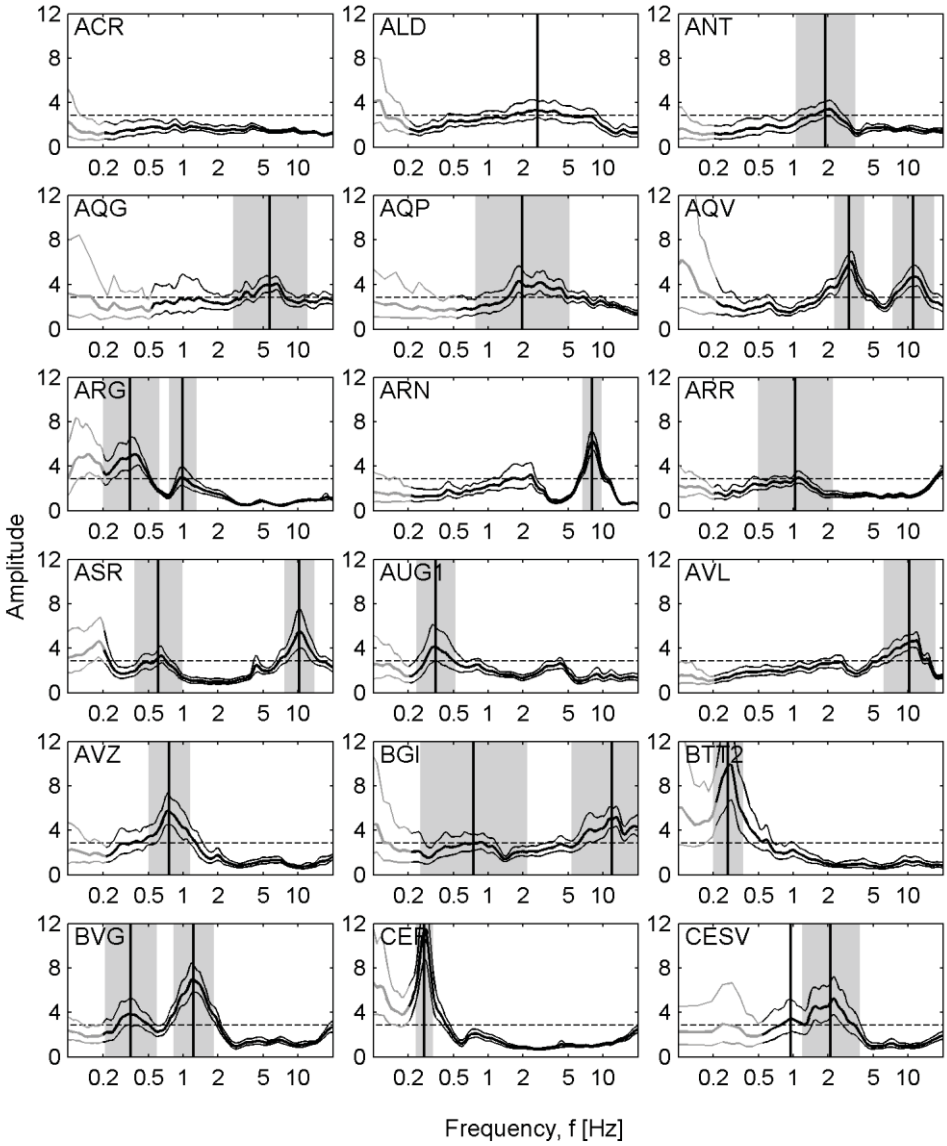

Fig. 8a - HVSR with microtremor measurement published in ITACA (cf. http://itaca.mi.ingv.it/ItacaNet/): vertical lines represent the estimate of the frequency at which a peak is present and the associated band-widths are displayed as grey areas only if $C_W < 0.6$ (cf. Table 2); dashed lines represent the threshold value A'. Through the station code reported in the panels a search in the ITACA database could be performed to easily retrieve the relevant measurement report (cf. Fig. 2).

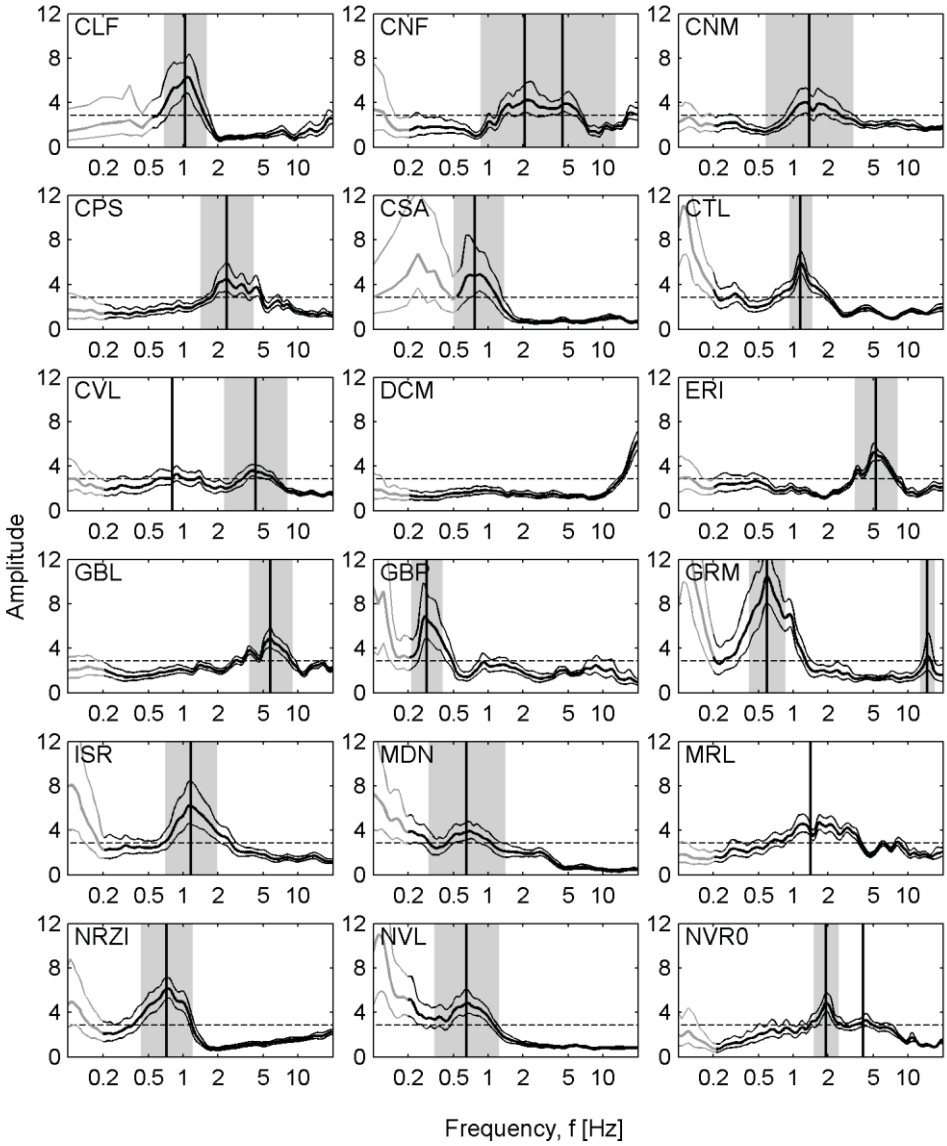

Fig. 8b - See previous caption.

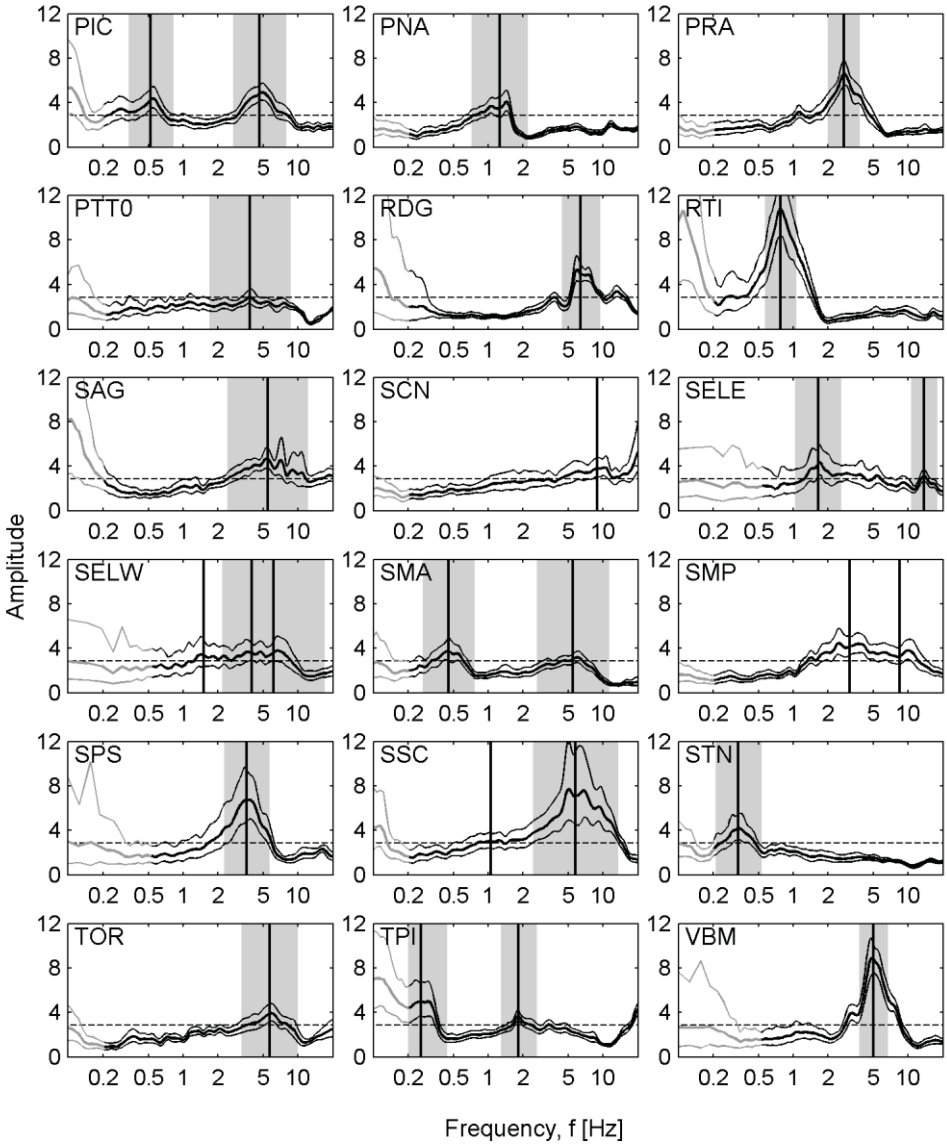

Fig. 8c - See previous caption.

Table 2 - Values of f_0^*, $\bar{f}_1$, $\bar{f}_2$, C_W, $C_W/A(f_0^*)$ and *S* relevant to the HVSR curves in Figure 8. The station codes are the same as those reported in Figure 8 and in the database ITACA.

Station code	f_0^* [Hz]	$\bar{f}_1$ [Hz]	$\bar{f}_2$ [Hz]	C_W	$\frac{C_W}{A(f_0^*)}$	*S*	Station code	f_0^* [Hz]	$\bar{f}_1$ [Hz]	$\bar{f}_2$ [Hz]	C_W	$\frac{C_W}{A(f_0^*)}$	*S*
ACR	-	-	-	-	-	-	GBP	0.29	0.21	0.40	0.14	0.02	6
ALD	2.68	0.54	13.40	0.69	0.21	2	GRM	0.59	0.41	0.86	0.16	0.02	6
ANT	1.90	1.04	3.46	0.26	0.08	5		14.60	12.60	17.00	0.07	0.02	4
AQG	5.69	2.69	12.00	0.41	0.10	3	ISR	1.17	0.70	1.97	0.23	0.04	5
AQP	1.98	0.77	5.09	0.51	0.13	3	MDN	0.65	0.30	1.41	0.34	0.09	4
AQV	3.05	2.26	4.11	0.13	0.02	5	MRL	1.42	0.20	10.50	0.86	0.23	4
	11.00	7.24	16.6	0.18	0.04	5	NRZI	0.72	0.43	1.21	0.23	0.04	6
ARG	0.34	0.20	0.62	0.25	0.05	4	NVL	0.65	0.34	1.24	0.28	0.06	5
	0.98	0.75	1.30	0.12	0.04	6	NVR0	1.92	1.49	2.48	0.11	0.02	6
ARN	7.94	6.53	9.67	0.09	0.01	6		4.07	0.97	17.00	0.62	0.19	5
ARR	1.04	0.49	2.21	0.33	0.11	5	PIC	0.52	0.33	0.82	0.20	0.05	5
ASR	0.61	0.37	0.98	0.21	0.07	6		4.62	2.72	7.85	0.23	0.05	5
	10.20	7.59	13.80	0.13	0.02	5	PNA	1.25	0.71	2.21	0.25	0.07	5
AUG1	0.35	0.24	0.52	0.17	0.04	6	PRA	2.75	1.99	3.80	0.14	0.02	5
AVL	10.20	6.09	17.20	0.23	0.05	5	PTT0	3.80	1.67	8.61	0.35	0.12	3
AVZ	0.75	0.50	1.14	0.18	0.03	6	RDG	6.38	4.36	9.34	0.17	0.03	4
BGI	0.75	0.25	2.18	0.47	0.16	3	RTI	0.77	0.57	1.05	0.14	0.01	6
	11.90	5.24	20.00	0.29	0.06	3	SAG	5.43	2.42	12.20	0.35	0.08	3
BTT2	0.27	0.20	0.36	0.13	0.01	5	SCN	8.81	0.92	20.00	0.67	0.18	3
BVG	0.35	0.21	0.59	0.23	0.06	5	SELE	1.65	1.04	2.62	0.25	0.06	4
	1.22	0.82	1.83	0.17	0.03	6		13.70	10.60	17.70	0.14	0.05	3
CER	0.28	0.23	0.33	0.07	0.01	6	SELW	1.52	0.50	20.00	1.00	0.30	2
CESV	0.96	0.50	9.20	0.79	0.23	5		3.93	0.85	18.10	0.82	0.23	3
	2.12	1.19	3.75	0.31	0.06	5		6.07	2.17	16.90	0.56	0.15	3
CLF	1.04	0.67	1.60	0.23	0.04	5	SMA	0.45	0.27	0.76	0.23	0.06	5
CNF	2.08	0.86	5.06	0.39	0.09	4		5.43	2.62	11.20	0.32	0.11	4
	4.41	1.52	12.80	0.46	0.12	4	SMP	3.08	0.74	12.90	0.62	0.15	3
CNM	1.37	0.57	3.30	0.38	0.10	3		8.42	0.20	20.00	1.00	0.31	3
CPS	2.39	1.41	4.07	0.23	0.05	5	SPS	3.55	2.26	5.58	0.25	0.04	5
CSA	0.77	0.50	1.37	0.27	0.06	3	SSC	1.05	0.20	20.00	1.00	0.33	3
CTL	1.16	0.92	1.46	0.10	0.02	6		5.75	2.45	13.50	0.37	0.05	5
CVL	0.81	0.20	16.60	0.96	0.32	3	STN	0.33	0.21	0.53	0.20	0.05	5
	4.26	2.26	8.04	0.28	0.08	4	TOR	5.62	3.19	9.89	0.25	0.06	4
DCM	-	-	-	-	-	-	TPI	0.26	0.20	0.44	0.17	0.03	4
ERI	5.24	3.42	8.04	0.19	0.04	6		1.83	1.28	2.62	0.16	0.04	6
GBL	5.75	3.71	8.92	0.19	0.04	5	VBM	4.95	3.72	6.59	0.16	0.02	6

5. Comparison of HVSR estimates and independent evaluations of f_0

At present, the ITACA database contains information about the shear wave velocity profile of more than 100 sites of the Italian accelerometric networks, 60 of which were characterized in the framework of the Italian Strong Motion Database project using different geophysical techniques (Foti *et al.*, this issue). A significant part of these profiles were *a priori* excluded from the comparison because they were obtained by also considering HVSR curves measured at the

relevant sites or other ambient vibration measurements (e.g. from 2D arrays). For the sites where a shear wave velocity profile obtained with methods independent from HVSR technique reaches the bedrock, i.e. velocity greater than 800m/s – as prescribed for rock-like geological formation by EuroCode8 (ENV, 2002) –, the 1D theoretical site response for SH waves was calculated by Luzi *et al*. (this issue) assuming a linear behaviour of the soil (Haskell, 1950; Thomson 1953). Only 9 sites were selected having a HVSR measurement that clearly indicates a f_0, and a shear wave velocity profile which reaches the bedrock. The resonant frequency value obtained with microtremor measurements ($f_{0,HVSR}$) and 1D modelling carried on by considering the relevant Vs profile ($f_{0,1D\text{-}sim}$) are thus compared in Figure 9. In general, there is a good agreement between the two sets of values, with few exceptions, such as SELE ($f_{0,HVSR} \cong 2$Hz; $f_{0,1D\text{-}sim} \cong 7$Hz) and BGI ($f_{0,HVSR} \cong 10$Hz; $f_{0,1D\text{-}sim} \cong 5$Hz). The measurements at these stations have been classified as B class – medium quality – (SELE) and C – low quality – (BGI). In addition, the station SELE could be affected by 2D amplification phenomena, due to its topographic setting.

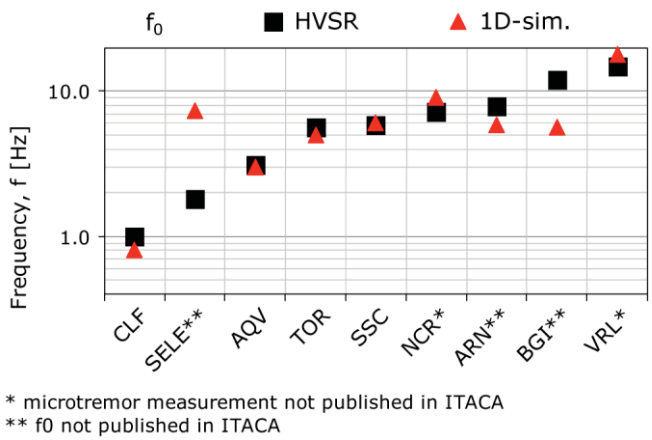

Fig. 9 - Comparison between f_0 from microtremor and from 1D modeling at accelerometric stations for which a noise measurement and an independent shear wave velocity profile down to the bedrock are available. The following geophysical tests were conducted for each station: CLF, down-hole (Di Giulio *et al*., 2006); SELE, down-hole (Capilleri *et al*., 2005); AQV, MASW and cross-hole (Luzi *et al*., 2010); SSC, down-hole (Programma VEL; *OPCM 3362/06*); TOR and VRL, MASW (DPC-INGV S4 2007-2009, http://esse4.mi.ingv.it); NCR, down-hole (Bozzano *et al*., 2000); ARN and BGI, cross-hole (ISMES, 1992; *Progetto Irpinia, Allegato 6*; NERIES Project, http://www.neries-eu.org/).

Luzi *et al*. (this issue) also computed the f_0 from the ratio between the horizontal and the vertical component of the acceleration response spectra (5% damping) for the stations with more than 2 earthquake records (cf. Lermo and Chavez Garcia 1993; Yamazaki and Ansary, 1997; Zhao *et al*., 2006). In Figure 10 they are compared with the f_0 obtained from the microtremor measurements. The results are also in good agreement, demonstrating the effectiveness of the procedure adopted for the identification and characterization of resonance phenomena at the accelerometric stations using ambient vibration. It should be noticed that the f_0 estimated for the site SELE, through the response spectra ratios of earthquakes, furnishes a result in agreement with that from microtremor measurement; it could arise doubts about the actual reliability of the shear wave velocity profile used to compute $f_{0,1D\text{-}sim}$ in Figure 9.

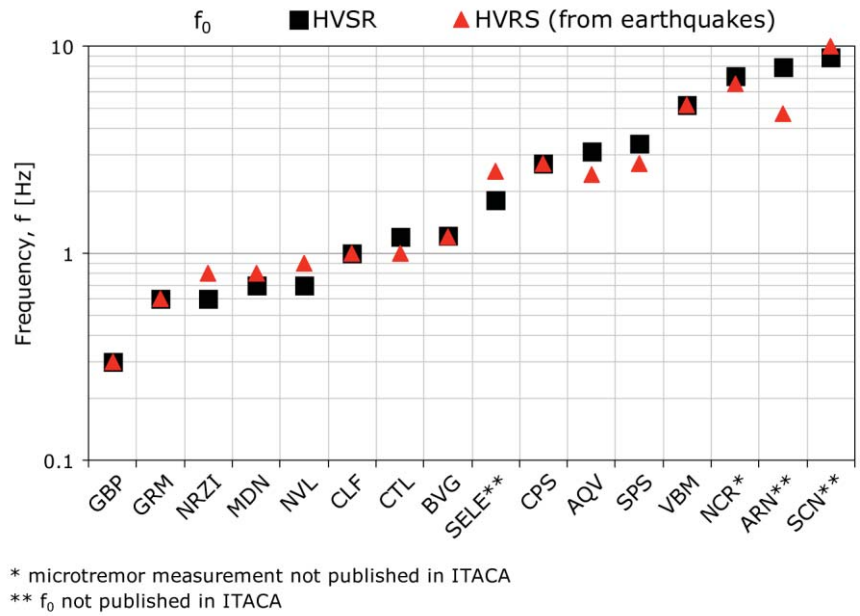

Fig. 10 - Comparison between f_0 from microtremor and from response spectra ratio of earthquake recordings. The recordings of NRC station are assumed for station NRZI.

The HVSR curves, whose f_0 are reported in Figures 9 and 10, are also displayed in Figure 8, with the exception of NCR and VRL, for which microtremor measurements were not published in ITACA. Furthermore, the shear wave velocity profiles, used for 1D simulations of Figure 9, are also reported in the relevant ITACA monographs, with the exceptions of BGI and ARN.

6. Conclusion

This paper describes the protocol developed to process and validate in a standardized way single station ambient vibration measurements (HVSR approach) carried on at a set of sites of the Italian Accelerometric network. In particular, a new effective numerical procedure to automatically detect resonance phenomena affecting Italian accelerometric stations has been developed and applied. Since seismic resonance phenomena can significantly affect the recordings of earthquakes, availability of this protocol could be of great importance for an extensive correct characterization of accelerometric records to be considered for engineering and seismological applications.

The feasibility of the proposed procedure was tested on more than 200 ambient vibration measurements, collected in the framework of the Italian Strong Motion Database project (DPC-INGV 2007-2009 S4; http://esse4.mi.ingv.it). In the analyses, particular attention was paid to the evaluation of the quality of the measurements embracing the criteria proposed by Albarello *et al*. (2011), since several sites were not characterized by geological-geotechnical information to adequately constrain the HVSR results. A key point of the proposed approach regards to the estimation of the fundamental frequencies of a site. In particular, a robust numerical procedure to uniquely estimate the peaks from an empirical HVSR curve is proposed.

The reliability of the estimated fundamental frequencies provided in this way was tested for those stations where estimates obtained with independent methods (numerical simulations or earthquake recordings) were available. The test

confirmed the reliability of the interpretation of high quality microtremor measurements in assessing the fundamental frequencies at the examined sites. This study shows that, low-cost measurements such as ambient vibrations can provide reliable indications on the fundamental frequencies of the subsoil at the accelerometric stations for which earthquake recordings are not available.
Information collected and processed with the protocol described above (including data processing, quality determination, estimates of the fundamental resonance frequencies from ambient vibration measurements) are available on the ITACA database (http://itaca.mi.ingv.it/ItacaNet/) in the form of station monographs also including further relevant data (local morphologic, geological characterization, Vs profile, geotechnical information, etc.).

Acknowledgements

This study has been carried on in the framework of the Italian Strong Motion Database project (DPC-INGV S4 2007-2009; http://esse4.mi.ingv.it). The Authors wish to thank: Dr. Riccardo Mario Azzara (INGV, Arezzo), Dr. habil. Stefano Parolai (GFZ, Potsdam) and Dr. Giuliano Milana (INGV, Roma), for their helpfulness in providing us the microtremor measurements acquired by their institutions. A fundamental help was given by Dr. Dino Bindi (INGV, Milano; GFZ, Potsdam), who kindly gave precious advices in ambient vibration data processing.

References

Albarello D. and Lunedei E. (2010) Alternative interpretations of horizontal to vertical spectral ratios of ambient vibrations: new insights from theoretical modeling. Bull Earthquake Eng, 8, 519-534. doi:10.1007/s10518-009-9110-0

Albarello D., Cesi C., Eulilli V., Guerrini F., Lunedei E., Paolucci E., Pileggi D., Puzzilli L.M. (2011) The contribution of the ambient vibration prospecting in seismic microzoning: an example from the area damaged by the 26th April 2009 l'Aquila (Italy) earthquake, Boll Geofis Teor Appl (in press)

Albarello D., and Lunedei E., (2011) Structure of ambient vibration wavefield in the frequency range of engineering interest ([0.5, 20] Hz): Insights from numerical modelling. Near Surface Geophysics, 9, doi:10.3997/1873-0604.2011017

Bard P.Y. (1999) Microtemor measurements: a tool for site effects estimation? In: The effects of surface geology on seismic motion. Irikura K., Kudo K., Okada H., Sasatani T. (editors). Balkema, Rotterdam, 1251-1279

Bonnefoy-Claudet S., Kö hler A., Cornou C., Wathelet M., Bard P.Y. (2008) Effects of Love waves on microtremor H/V ratio. Bull Seism Soc Am, 98, 1, 288-300

Bonilla L.F., Steidl J.H., Lindley G.T., Tumarkin A.G., Archuleta R.J. (1997) Site amplification in the San Fernando Valley, California: Variability of site-effect estimation using the S-wave, coda, and H/V methods. Bull Seism Soc Am, 87, 710-730

Bozzano F., Tento A., Larotonda A. (2000) Microzonazione di Nocera Umbra. In: Terremoto dell'Umbria-Marche. Cattaneo M., Marcellini A. (editors), CNR-GNDT, Rome, 71-138 (in italian)

Cadet H., Bard P.Y., Duval A.M. (2008) A new proposal for site classification based on ambient vibration measurements and the Kiknet strong motion data set. Proceeding of The 14th World Conference on Earthquake Engineering, October 12-17, 2008, Beijing, China

Cadet, H., Bard P.Y., Rodriguez-Marek A. (2010) Defining a standard rock site: proposition based on the KiK-net database. Bull Seism Soc Am, 100, 1, 172-195. doi: 10.1785/0120090078

Capilleri P., Lanzo G., Maugeri M., Pagliaroli A. (2005) Site effects evaluation in Sellano (Italy) by 1-D and 2-D numerical analyses. In: Earthquake Resistant Engineering Structures V. C.A. Brebbia, D.E. Beskos, G.D. Manolis, C.C. Spyrakos (editors), WIT Press, Southampton, 73-82. ISBN: 1-84564-018-7

Chávez-García F.J., Raptakis D., Makra K., Pitilakis K. (2002) Importance of the reference station in modeling site effects up to larger frequencies. The case of Euroseistest, 12th European conference on earthquake engineering, paper reference 589, London, 2002.
D'Amico V., Picozzi M., Baliva F. and Albarello D. (2008) Ambient Noise Measurements for Preliminary Site-Effects Characterization in the Urban Area of Florence. Bull Seism Soc Am, 98, 3, 1373-1388, June 2008, doi: 10.1785/0120070231
Di Giulio G., Cornou C., Ohrnberger M., Wathelet M., Rovelli A. (2006) Deriving Wavefield Characteristics and Shear-Velocity Profiles from Two-Dimensional Small-Aperture Arrays Analysis of Ambient Vibrations in a Small-Size Alluvial Basin, Colfiorito, Italy. Bull Seism Soc Am, 96(5): 1915-1933
ENV 1998-1-1 (2002) EUROCODE 8, Design Provisions for Earthquake Resistance of Structures. Seismic Actions and General Requirements of Structures, CEN/TC 250, Draft, May 2002
Forbriger T. (2006) Low-frequency limit for H/V studies due to tilt. Extended Abstract. 32. Sitzung der Arbeitsgruppe Seismologie des FKPE. Haidhof, Germany
Fukushima Y., Bonilla L.B., Scotti O., Douglas J. (2007) Site Classification Using Horizontal-to-vertical Response Spectral Ratios and its Impact when Deriving Empirical Ground-motion Prediction Equations. Journal of Earthquake Engineering, 11, 5, 712-724
Haghshenas E, Bard P-Y, Theodulidis N, SESAME WP04 Team (2008) Empirical evaluation of microtremor H/V spectral ratio. Bull Earthquake Eng 6, no. 1, 75-108.
Haskell N. A. (1953) The dispersion of surface waves on multilayered media. Bull Seism Soc Am, 43, 17–34.
Japan Road Association (1980) Specifications for Highway Bridges Part V. Seismic Design. Maruzen Co., LTD.
Konno K., Ohmachi T. (1998) Ground-Motion Characteristics Estimated from Spectral Ratio between Horizontal and Vertical Components of Microtremor. Bull Seism Soc Am, 88, 228-241.
Lachet C., Hatzfeld D, Bard P.-Y., Theodulidis N., Papaioannou C., Savvaidis A. (1996) Site effects and microzonation in the city of Thessaloniki (Greece) comparison of different approaches. Bull Seism Soc Am, 86, 1692-1703
Lermo J., Chávez-García F.J. (1993) Site effect evaluation using spectral ratios with only one station. Bull Seism Soc Am, 83, 1574-1594
Lunedei E., Albarello D. (2010) Theoretical HVSR from the full wave field modelling of ambient vibrations in a weakly dissipative layered Earth. Geophys J Int, 181, 1093-1108, doi: 10.1111/j.1365-246X.2010.04560.x
Luzi L., Lovati S., D'alema E., Marzorati S., Giacomo D., Hailemikael S., Cardarelli E., Cercato M., Filippo G., Milana G., Giulio G., Rainone M., Torrese P., Signanini P., Scarascia Mugnozza G., Rivellino S., Gorini A. (2010) Italian accelerometric archive: geological, geophysical and geotechnical investigations at strong-motion stations. Bull Earthquake Eng, vol. 8 (5) pp. 1189-1207
Manakoua M.V., Raptakisa D.G., Chávez-Garcíab F.J., Apostolidisa P.I., Pitilakisa K.D. (2010) 3D soil structure of the Mygdonian basin for site response analysis. Soil Dyn Earthq Eng 30, 11, 1198-1211. doi:10.1016/j.soildyn.2010.04.027
Nakamura Y. (1989) A method for dynamic characteristics estimation of subsurface using microtremor on the ground surface. QR Railway Tech. Res. Inst., 30, 25-33
Nogoshi M., Igarashi T. (1971) On the amplitude characteristics of microtremor (part 2). J Seism Soc Japan, 24, 26-40
Parolai S., Bormann P., Milkereit C. (2001) Assessment of the natural frequency of the sedimentary cover in the Cologne area (Germany) using noise measurements. Journal of Earthquake Engineering, 5, 4, 521-539
Steidl J., Tumarkin A., Archuleta R. (1996) What Is a Reference Site? Bull Seism Soc Am, 86(6):1733-1748
Thomson W. T. (1950) Transmission of elastic waves through a stratified solid media, J Appl Phys 21, 89–93
Site Effects Assessment using Ambient Excitations (SESAME) European project (2005) Deliverable D23.12 - Guidelines for the implementation of the H/V spectral ratio technique on ambient vibrations: measurements, processing and interpretation. http://sesame-fp5.obs.ujf-grenoble.fr (accessed March 2010)
Yamazaki F., Ansary M.A. (1997) Horizontal-to-vertical spectrum ratio of earthquake ground motion for site characterization. Earthquake Eng Struct Dyn 26, 671-689
Zhao J.X., Irikura K., Zhang J., Fukushima Y., Somerville P.G., Asano A., Ohno Y., Oouchi T., Takahashi T., Ogawa H. (2006) An Empirical Site-Classification Method for Strong-Motion Stations in Japan Using H/V Response Spectral Ratio. Bull Seism Soc Am, 96, 914-925

References to this issue

Foti S., Parolai S., Bergamo P., Di Giulio G., Maraschini M., Milana G., Picozzi M., Puglia R.: Surface wave surveys for seismic site characterization of accelerometric stations in ITACA

Luzi L., Puglia R., Pacor F., Gallipoli M.R., Bindi D., Mucciarelli M.: Proposal for a soil classification based on parameters alternative or complementary to $V_{S,30}$